Journal of Inorganic Biochemistry 199 (2019) 110799

Contents lists available at ScienceDirect

Journal of Inorganic Biochemistry

journal homepage: www.elsevier.com/locate/jinorgbio

Brain oxidative stress in rat with chronic iron or copper overload

R. Musacco Sebio[a], N. Ferrarotti[b], F. Lairion[a], C. Saporito Magriñá[a], J. Fuda[c], H. Torti[c], A. Boveris[a,d], M.G. Repetto[a,d,*]

[a] Universidad de Buenos Aires, Facultad de Farmacia y Bioquímica, Departamento de Química Analítica y Fisicoquímica, Cátedra de Química General e Inorgánica, Argentina
[b] Universidad de Buenos Aires, Facultad de Farmacia y Bioquímica, Departamento de Bioquímica Clínica, Laboratorio de Autoinmunidad, Argentina
[c] Universidad de Buenos Aires, Facultad de Farmacia y Bioquímica, Departamento de Fisicomatemática, Cátedra de Física, Argentina
[d] Consejo Nacional de Investigaciones Científicas y Técnicas (IBIMOL, UBA-CONICET), Argentina

ARTICLE INFO

Keywords:
Iron
Copper
Brain oxidative stress
Glutathione
Metal dyshomeostasis
Wilson's disease

ABSTRACT

Male rats of 80–90 g that were fed 42 days with a commercial rodent diet of 2780 kcal/100 g and received chronic overloads of either Fe(II) or Cu(II) in the drinking water. The two metals produced brain oxidative stress and damage with marked increases in the indicators of oxidative processes: *in vivo* brain surface chemiluminescence (the sensitive organ non-invasive assay for oxidative free radical reactions), and the *ex vivo* processes of phospholipid peroxidation and protein oxidation. Brain redox imbalance was also indicated by marked decreases in the cellular indicators of oxidative metabolic stress: reduced glutathione (GSH) content and reduced/oxidized glutathione ratio (GSH/GSSG). Brain decreased GSH content has a central role in the biochemical oxidative processes associated with Fe and Cu chronic damage. The understanding of biochemical oxidative imbalances in the rat brain with chronic Fe(II) or Cu(II) overloads may be useful for the establishment of pharmacological therapies for human pathologies associated to Fe and Cu cellular imbalances.

1. Introduction

Elevated brain levels of iron (Fe) and copper (Cu) have been associated with the onset and progression of several neurodegenerative diseases. It has been recognized that Fe and Cu disturbances in brain metabolism and homeostasis could be linked to the incidence and progression of neurodegenerative diseases and of the cognitive disorders associated with aging [1–4]. The processes of free radical generation and of protein aggregation are involved in the establishment of neuronal oxidative stress and damage. In general terms, it is understood that the metals generate an intracellular oxidizing environment that leads to an increased formation of hydroxyl radical ($HO^{\bullet}$) through the Fenton/Haber-Weiss reaction [5], which immediately leads to intracellular oxidative damage with increases in the processes of phospholipid peroxidation and of protein oxidation and decreases in thiol group (-SH) content. In the cytosol of brain neurons, the mentioned oxidative processes involve a shift towards the oxidation of -SH groups accompanied by the misfolding of newly synthesized macromolecules and by the formation of protein aggregates, as observed in Alzheimer's, Parkinson's and prion diseases [6].

It has been claimed that brain neuronal Fe(II) reacts with α-synuclein (the main protein component of Lewis bodies in Parkinson's disease) and with the β-amyloid peptide (Aβ) in the extracellular plaques of the cerebral cortex of Alzheimer's disease patients and leads to neuronal oxidative damage that contributes to disease progression [7–9]. A positive correlation has been found between Fe dyshomeostasis and the generation of amyloid plaques, which are characteristic of the affected brains of patients with Alzheimer's disease [10–12]. In Parkinson's disease, excessive Fe was found in *substantia nigra pars compacta,* an area where dopaminergic neurons are exposed to high levels of superoxide anion (O_2^{-}) and hydrogen peroxide (H_2O_2) from dopamine oxidation [10]. Thus, excess intracellular Fe(II) and Cu(II) catalyzes the formation of $HO^{\bullet}$ radical from H_2O_2 and impairs neuronal metabolism and intracellular signaling by oxidative damage.

The development of chelation therapy, which is based on the complexation and inactivation of neuronal cytosolic Fe and Cu, has gained interest as part of new strategies in the treatment of neurodegenerative diseases [13–15].

Cu is an essential metal which participates in several biological reactions. However, due to its high reactivity it is also potentially toxic

* Corresponding author at: Universidad de Buenos Aires, Facultad de Farmacia y Bioquímica, Cátedra de Química General e Inorgánica, Junín 956, 1113AAD Buenos Aires, Argentina.
E-mail address: mrepetto@ffyb.uba.ar (M.G. Repetto).

https://doi.org/10.1016/j.jinorgbio.2019.110799
Received 26 March 2019; Received in revised form 5 August 2019; Accepted 5 August 2019
Available online 06 August 2019
0162-0134/

for the cell [16]. Intracellular Cu facilitates the formation of the amyloid plaques characteristic of Alzheimer's disease by increasing the formation and accumulation of the Aß from the amyloid precursor protein (APP) [17]. Cu binds to Aß and to APP, where it is reduced [18,19]. It seems that Cu(I) and Cu(II) contribute to the formation of cross-links between proteins and to the aggregation of amyloid plaques. The insoluble amyloid plaques in post-mortem brains of Alzheimer patients show elevated levels of Cu, Fe and Zn [17].

Another piece of information about increased Cu levels and brain dysfunction is found in Wilson disease (caused by mutations in the Cu-transporting adenosine triphosphatase (ATPase) ATP7B gene with reduced excretion of Cu into the bile). An important part, 40–50%, of these Wilson disease patients simultaneously shows liver Cu accumulation and neurological and neuropsychiatric symptoms, such as tremor, ataxia, dystonic syndrome, depression, anxiety and psychosis. Patients intoxicated with Cu show hepatic disease ranging from mild hepatitis to acute liver failure or cirrhosis.

Increased levels of Cu in the body fluids lead to brain dysfunction and structural damage as observed in brain areas (putamen, globus pallidus, caudate, thalamus, midbrain and cerebellum) of patients with Wilson disease. In patients with liver Cu accumulation, neurological symptoms are slow and appear after 2–5 years. Some patients with neurological signs show asymptomatic liver disease [19].

The Fe(II) and Cu(II) doses employed in this study, which focuses on brain oxidative stress, were equal to the ones used in a previous study in rat liver [20]. Such Fe(II) and Cu(II) doses decreased the animal survival to 98% and 72% respectively, after 42 days [20]. A slight decrease in animal growth was also observed. By the end of the treatments, rat weights were: controls 376 ± 4 g; Fe-overload 360 ± 3 g; and Cu-overload 328 ± 3 g [20].

Chronic overloads of Fe(II) and Cu(II) in rats led to accumulation of the metals in the brain associated with increased oxidative processes, redox dyshomeostasis and decreased intraneuronal reduced glutathione (GSH).

The rat model of Fe and Cu overloads should be useful to develop treatments to prevent the oxidative stress and organ damage in human pathologies associated with metal overloads and dysmetabolism.

2. Material and methods

2.1. Experimental Fe and Cu chronic overloads

Male Sprague-Dawley rats of 80–90 g were fed with a commercial rodent diet provided by the company GEPSA inscription SENASA0021/A manufactured by GRUPO PILAR S.A. 100 g of the commercial food has a minimum of protein content (24%), a minimum of ether extract (6%), a minimum (0.5%) and maximum (0.9%) of phosphorus content, maximum humidity of 13%, maximum fiber of 7%, minimum (1%) and maximum (1.2%) calcium content, and a maximum total mineral content (8%). Animals were fed *ad libitum* and received drinking water with either 1.0 g/L of $FeCl_2$ or 0.5 g/L $CuSO_4$ for 42 days. Control group received water without metals. Male rats were chosen because females have hormonal cycles that can modify certain biological responses. In previous studies of our group the experiments with acute overload of Fe or Cu were performed using male rats, therefore we continued with rats of the same sex for the study of chronic overloads. Animal care was given according to the Guidelines for Ethical Treatment in Animal Experimentation of the American Physiological Society (Bethesda, MD, USA), to Argentine regulations (ANMAT), and to the guide for Care and Use of Laboratory Animals of the Faculty of Pharmacy and Biochemistry, University of Buenos Aires (Res. D 3685/16). Rats were from the Animal House of the Faculty of Pharmacy and Biochemistry that were acclimatized to laboratory conditions 7 days before experiments. The animals were maintained at 23–25 °C with 50% humidity and with 12 h light–12 h dark cycles.

2.2. Brain metal content

The brain cortex samples were washed with ice cold saline solution until blood was completely removed. The content of Fe and Cu were determined by atomic absorption. The weighted samples were placed in a porcelain crucible with the addition of 1 mL of concentrated HNO_3 (68.1% *w*/w, density of 1.405 g/mL) and then placed on a heating plate until the colored fumes are no longer observable. After that, the treated residue was placed in a heating furnace and heated at 500 °C for one hour. Finally, the ashes were dissolved by adding 2 mL of HCl 50% *v*/v. The brains are weighted in porcelain crucibles and heated at 90 °C to dry the tissue. Then, the samples are carbonized by gradually increasing the temperature as follows: 200 °C for one hour, 400 °C for one hour and finally 500 °C for one hour (these heating time intervals do not include the time required to heat and chill the samples). Whether there is still carbon in the samples, an additional volume of 1 mL 50% *v*/v HNO_3 is added to the crucible and the samples are heated slowly in a muffle furnace to oxidize the organic matter. Finally, the samples are heated for an additional hour at 500 °C. Standard solutions of 0–3 mg/L were used for calibration. Determinations were made in an atomic absorption spectrometer (Bück model 200A, East Norwalk, CT, USA) and results were expressed in µg of metal/g of wet brain [20,21].

2.3. Brain chemiluminescence

Brain surface chemiluminescence, the *in vivo* organ non-invasive assay for free-radical reactions, was determined following previously used protocols [22–24]. Brain chemiluminescence integrates both the oxidative process and the antioxidant response. Spontaneous organ chemiluminescence reports in real time the steady state level of singlet oxygen ($^1O_2$), the electronically excited state of oxygen (O_2). $^1O_2$ reports on the rate of phospholipid peroxidation process, because it is produced after the collision of two ROO'to form the instantaneously broken intermediate ROOOOR [22]. The photon counter was designed and constructed by Prof. Britton Chance at the Johnson Research Foundation of the University of Pennsylvania (Philadelphia, PA, USA) [22]. Brain chemiluminescence was expressed in counts per second per cm^2 (cps/cm^2) of exposed brain surface. The skull of anesthetized rats was open and washed with 0.9% NaCl to remove blood. Brain was exposed and the animal covered with aluminum foil, in which a 2–3 cm^2 window allowed brain exposure to the detector. Brain surface chemiluminescence was measured after stable photoemission readings (usually 2–3 min) and recorded for 2–3 min. After that, brain was excised for the *ex vivo* determinations of oxidative damage.

2.4. Brain homogenate preparation

Rat brain cortex was rapidly excised, weighed and cut into small pieces of 2–3 mm that were washed with ice cold saline solution until blood was completely removed. The homogenate was prepared in 120 mM KCl, 30 mM phosphate buffer, pH 7.40, at a ratio of 9.0 mL solution/g of tissue at 0–1 °C in an ice bath. The suspension was passed through a small Potter-Elvehjem homogenizer and then centrifuged (Sorvall RC-2B, rotor SS34, 2500 rpm) at 600*g* for 10 min and at 0–1 °C. The supernatant, constituted by a suspension of organelles and cell cytosol, was considered as brain homogenate and was stored at −80 °C. The pellet, constituted by cell debris, was discarded [25,26]. For the determinations of GSH content and reduced/oxidized glutathione ratio (GSH/GSSG), small pieces of 1–2 mm of brain were added with 0.5 M $HClO_4$ at a ratio of 50 mL $HClO_4$/g of tissue. The suspension was passed through a Potter-Elvehjem homogenizer and centrifuged at 600*g* for 10 min. The pellet was discarded and the supernatant stored at −80 °C for further determinations. The whole procedure was carried out at 0–1 °C.

2.5. Phospholipid peroxidation

Thiobarbituric acid reactive substances (TBARS) were determined. For this purpose, 1.0 mL of brain homogenate was added with 0.1 mL 4% *w/v* butylhydroxytoluene in ethanol and the samples were deproteinized by addition of 1 mL 20% w/v trichloroacetic acid and 10 min centrifugation in a table centrifuge. The supernatant was passed to a test tube and added with 1.0 mL of 0.7% w/v thiobarbituric acid. The tubes were vortexed and heated in a boiling water bath for 30 min. The absorbance of the pink solution was measured at 535 nm ($\varepsilon = 156\ mM^{-1}\ cm^{-1}$) and the results were expressed as nmol TBARS/g of brain [20,27].

2.6. Protein oxidation

Protein oxidation was measured by the conjugation of protein carbonyl groups (> C=O) with 2,4-dinitrophenylhydrazine (DNPH) and determined spectrophotometrically at 360 nm. 1 mL of tissue homogenate was added with 4 mL of 10 mM DNPH prepared in 2.5 M HCl. Controls without brain homogenates were performed. Tubes were incubated for 1 h at room temperature in the dark and vortexed every 15 min. Then, 5 mL of 20% trichloroacetic acid were added to each tube and left in an ice bucket for 10 min. After that, samples were centrifuged in a tabletop centrifuge for 5 min to obtain the protein precipitates. The supernatant was discarded. 4 mL of 10% trichloroacetic acid were added to the pellet which was mechanically broken with a glass rod. The suspension was centrifuged for 5 min and the pellet was twice washed with 4 mL of a mixture of 1:1 ethanol-ethyl acetate to remove free DNPH and lipid contamination. Finally, the protein pellet was dissolved in 2 mL of 6 M guanidine, added with 4 mL of 10 mM DNPH and incubated for 10 min at 37 °C. The absorbance at 360 nm was determined in a spectrophotometer (Hitachi, model U-2000) [20,28]. As about 10–15% of proteins are lost in the washing steps, a calibration curve was used using serum albumin (0.2–0.6 mg) dissolved in 0.4 mL of 6 M guanidine as a marker of protein loss [28].

2.7. Oxidative damage index

The oxidative damage index estimates the degree of brain oxidative damage considering three markers (brain chemiluminescence, phospholipid peroxidation and protein oxidation) of oxidative processes. The indicators are taken as ratios of experimental and control values for each time point, the oxidative stress index indicates a global representation of the biomarkers of oxidative damage [29,30].

2.8. GSH and the GSH/GSSG ratio

Brain homogenate samples (1 mL) were added with 1 mL 0.5 M perchloric acid and neutralized with 2 M KOH. After centrifugation, GSH was measured in the supernatant in 100 mM phosphate buffer (pH 7.20) by its reaction with 70 μM 5,5′-dithio-vis-(2-nitrobenzoic acid), Ellmans's reagent (DTNB) to give a yellow-colored compound ($\varepsilon_{412} = 13.5\ mM^{-1}\ cm^{-1}$). GSSG was measured by the consumption of 0.2 mM reduced nicotinamide dinucleotide phosphate (NADPH) and 0.2 U/mL glutathione reductase [20,29,31]. Brain GSH content was expressed in mM, considering 1.0 g of brain as 0.8 mL of water.

2.9. Protein determination

Protein contents were measured by the Folin reagent using bovine serum albumin as standard.

2.10. Statistical analysis

All the results are expressed as mean ± standard error of the mean (SEM). Statistical analyses were carried out with Graphpad InStat following the recommended software settings for the present experiments (Anova with Tukey's post-test). The curve fitting were made using the Sigma Plot program for windows, version 11.0, Systat Software Inc., and the curve fitting was done with Dynamic Fit Wizard. The linear correlation between two variables was estimated with the Pearson correlation coefficient), calculated with the standard Pearson's formula by using the program SigmaPlot program for windows, version 11.0, Systat Software, Inc. Differences were considered statistically significant at $p < 0.05$.

2.11. Chemicals

Chemicals were purchased from Sigma-Aldrich Chemical Co, St Louis, Mo.

3. Results

The Fe and Cu accumulation kinetics showed marked increases in brain metal content during the overload period. By the end of the treatment, brain Fe content was increased by 400% from the initial level of 35 ± 5 μg Fe/g brain and brain Cu content was increased by 3600% from the basal content of 3.6 ± 0.8 μg Cu/g. The increases in brain Fe and Cu were roughly linear during treatments, the curve fitting algorithm, f(x) = metal content/time, was used with 95% confidence intervals (Fig. 1). A positive correlation was found between brain metal contents and the time of treatment ($r^2 = 0.97$ and 0.95 for Fe and Cu, respectively, $p < 0.05$).

Brain surface chemiluminescence *in vivo* was markedly increased from the initial value of 11 ± 2 cps/cm^2 in Fe(II) or Cu(II) overloads. The increases were sigmoidal and reached a maximum of 12-fold for Fe and 6-fold for Cu at day 7 (Fig. 2). It is worth recalling that organ surface chemiluminescence is a sensitive physiological assay for free-radical reactions *in vivo*.

The products of phospholipid peroxidation, measured as TBARS, were significantly increased in the overloads with Fe(II) and Cu(II), with maximal increases of 150% and 62% respectively at day 2 (Fig. 3) ($p < 0.01$) (Fig. 3). In brain, TBARS content showed a biphasic behavior for both metals overload, an initial response with increments that follow a sinusoidal function, with linear trend from day 4 to day 21 ($r^2 = 0.91$ and $r^2 = 0.99$ for Fe(II) and Cu(II) respectively), increasing steadily to the maximal value and then decreasing (p value between days 21 and 28 was 0.0012 for Fe, considered very significant, and 0.0005 for Cu, considered extremely significant), and remains constant

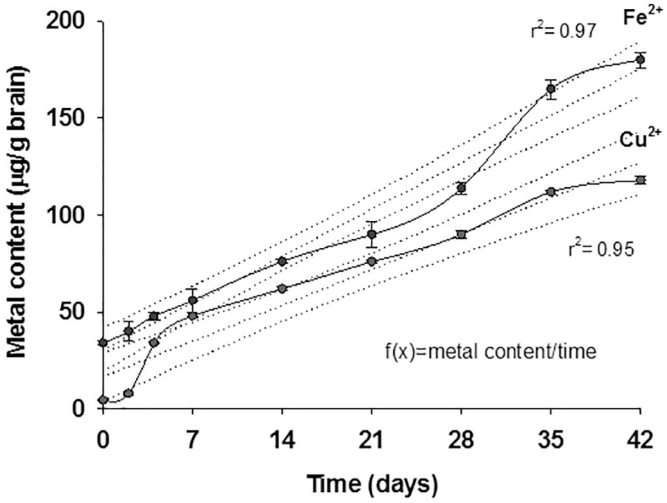

Fig. 1. Time profile of the brain contents of Fe and Cu during the chronic administration of either Fe(II) or Cu(II) in the drinking water for 42 days (** $p < 0.01$).

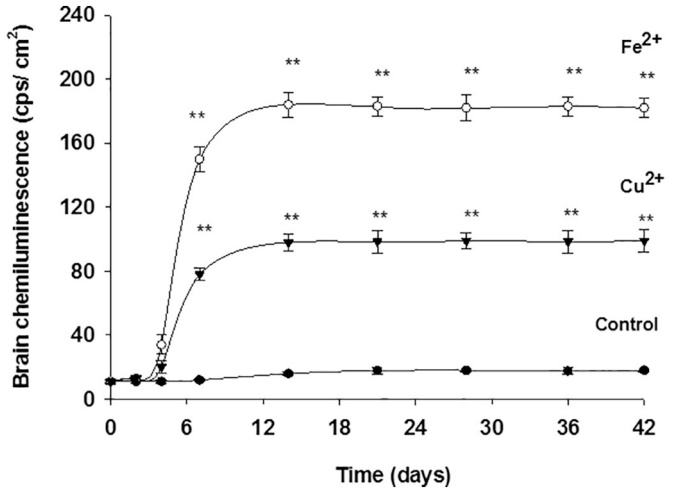

Fig. 2. Time profile of rat brain surface chemiluminescence *in situ* and *in vivo* in the chronic overloads with Fe(II) and Cu(II) (** p < 0.01).

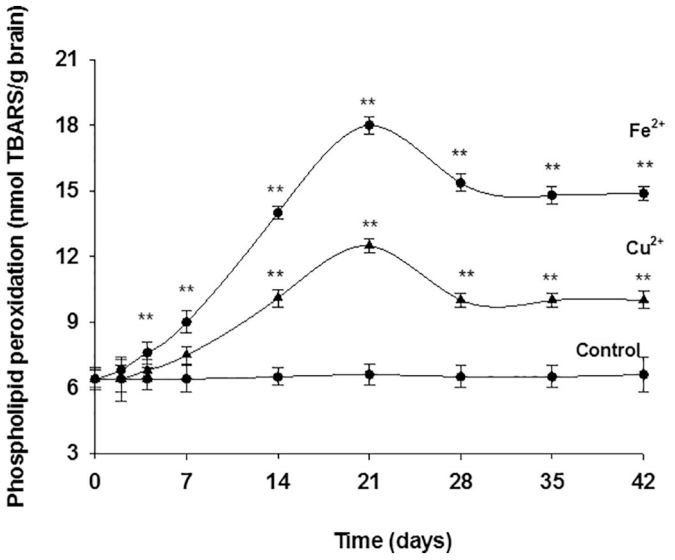

Fig. 3. Time profile of phospholipid peroxidation in rat brain determined as TBARS in the chronic overloads with either Fe(II) or Cu(II) (** p < 0.01).

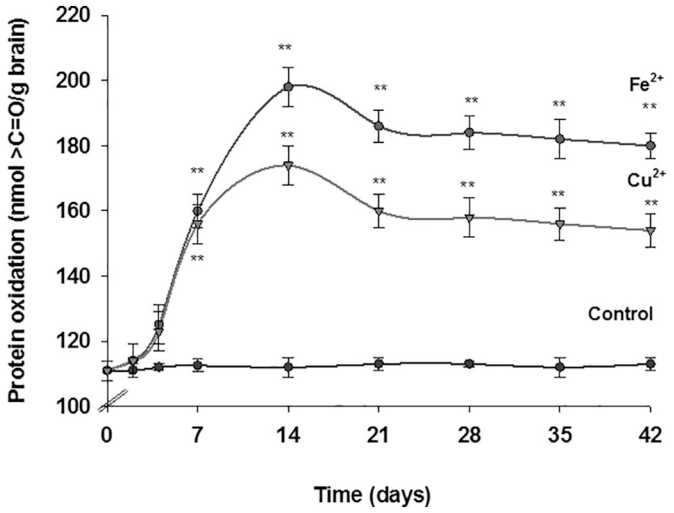

Fig. 4. Time profile of brain protein oxidation measured as carbonyl groups (> C = O) in the chronic overload with either Fe(II) or Cu(II) (* $p < 0.05$; ** p < 0.01).

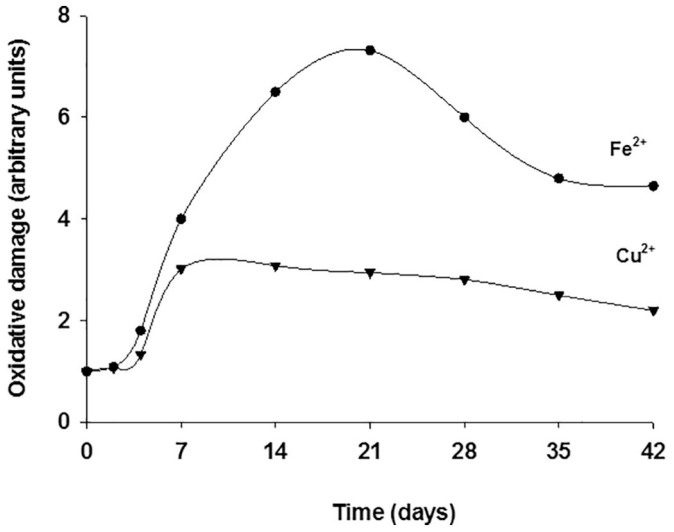

Fig. 5. Oxidative damage index in rat brain in the chronic treatments with either Fe(II) or Cu(II) overloads.

until day 42 (Fig. 3). Brain chemiluminescence correlated with phospholipid peroxidation up to day 7, remaining constant after that despite TBARS behavior. Apparently, it may be due to metabolic utilization of the products or synthesis of new phospholipids, as it was observed in rat liver in the chronic overloads with Fe(II) and Cu(II) [20].

The content of brain protein carbonyls also showed a biphasic behavior for both chronic overloads. An initial phase with sinusoidal shape and linear increment from day 4 to day 14 ($r^2 = 0.97$ for Fe and $r^2 = 0.93$ for Cu) which remained with constant values from 14 up to 42 days (Fig. 4), the same profile that was observed in brain chemiluminescence (Fig. 2). The maximal increments for protein carbonyl groups content were 77% for Fe(II) and 59% for Cu(II) overloads at day 14. After that, protein carbonyl content remained constant with Fe load (p value between days 14 and 21 was 0.0563, considered not quite significant) and decreased until reaching a *plateau* with Cu treatment from day 21 to day 42 (p value between days 14 and 21 was 0.0361 for Cu, considered significant). The determined values were well over the initial levels of 110 ± 3 nmol protein carbonyls/g brain.

The oxidative damage index increased significantly in both overloads, more marked for iron metal. Fe(II) supplementation increased the index by 600%, whereas Cu(II) overload augmented it 200%. Maximal values were observed at different times, appearing first in Cu (II) (days 7–21) than Fe(II) overloads (days 14–28), with a decrease at the end of the experiments (Fig. 5).

GSH content in the control group (2.8 ± 0.4 mM) is in the normal range (2–4 mM) for brain cells. GSH is the main antioxidant molecule involved in intracellular redox regulation and control [31]. It was markedly decreased in the metal overloads; 36% with Fe(II) and 60% with Cu(II). These very low brain GSH concentrations were observed from days 7–14 to day 42 at the end of treatments (Fig. 6).

In both Fe(II) and Cu(II) overloads, the very sensitive index GSH/GSSG, since it is the ratio of reduced/oxidized of the same glutathione pool, was deeply decreased at days 3–7, with a constant level maintained afterwards. The decrease in the GSH/GSSG ratio was 38% and 64% with Fe(II) and Cu(II) respectively. This ratio remained below the control value (28 ± 1) during the 42 days of the treatment with both metals (Fig. 7).

A kinetic analysis of changes in rat brain, after Fe(II) and Cu(II) overloads, was performed in a time period of 0 to 20 days (Fig. 8). The selected period correspond to the time when maximal effects were observed and the analysis was made ordering from left to right and

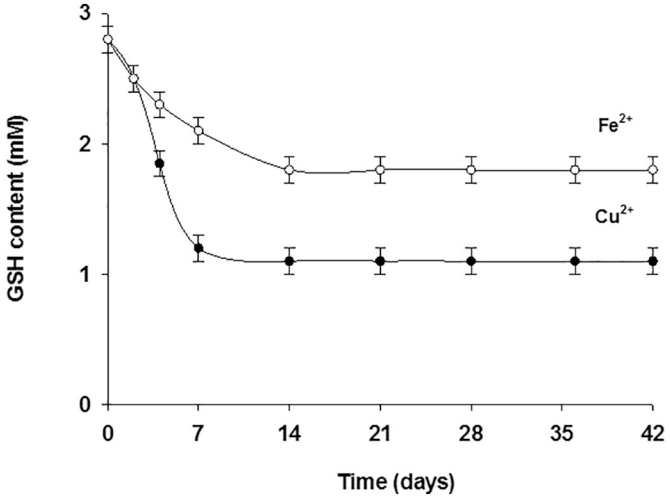

Fig. 6. Rat brain GSH content in the chronic overloads with either Fe(II) or Cu (II) (** $p < 0.01$).

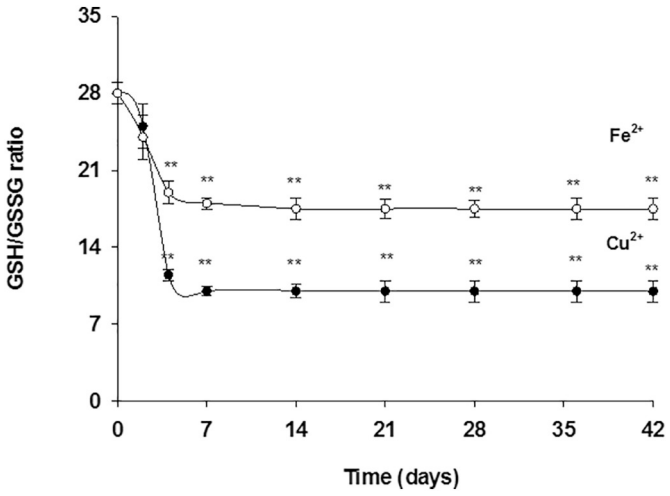

Fig. 7. Time profile of the GSH/GSSG ratio in rat brain during the chronic overloads with either Fe(II) or Cu(II) (** $p < 0.01$).

from faster to slower the reactions and processes, considering the time in which the considered indicators showed one-half change ($t_{1/2}$). This type of analysis illustrates the temporal sequence of the different oxidative processes and of the antioxidant defense. It also allows comparing the temporal sequence of oxidative and antioxidative processes in different organs of rats receiving chronic treatments with Fe (II) and Cu (II) in the drinking water (Fig. 8.).

In brain, as equal than in liver, the kinetics of the oxidative changes indicates that biomolecules oxidation takes place after the impairment of the GSH-dependent antioxidant defense. In brain, the time profile of biomolecules oxidation is different than in liver: protein oxidation is an early oxidative process in brain, whereas phospholipids are oxidized before than proteins in liver [20].

4. Discussion

The experimental data on the chronic Fe(II) and Cu(II) overloads in rats reported here showed clear evidence of brain oxidative damage. Increased levels of *in vivo* brain chemiluminescence (Fig. 2), increments in the *ex vivo* markers of phospholipid peroxidation (Fig. 3) and of protein oxidation (Fig. 4), and decreases in GSH content (Fig. 6) and in the GSH/GSSG ratio (Fig. 7) support the concept that oxidative processes mediated by free radicals are involved in the molecular mechanism of both Fe and Cu chronic brain damage.

The duration of the chronic treatment with Fe(II) or Cu(II) overloads in rats in this study is roughly equivalent to the length of a human treatment or situation of 6 years [20].

The chronic overloads of Fe(II) or Cu(II) reproduced the main oxidative phenomena that were previously observed in rat brain in acute Fe(II) or Cu(II) intoxications (15 mg/100 g rat for $FeCl_2$ or 5 mg/100 g rat for $CuCl_2$ in a single i.p. dose) and that were followed for 2 days [29,32]. Although the quantitative changes in oxidative indicators in the chronic and acute overloads are different they are qualitatively similar.

Due to the high metal intake in the drinking water, Fe and Cu build up steadily over time within rat brain with concomitant changes in several oxidative stress markers. These changes encompass the enhancement of biomolecule damage markers such as brain chemiluminescence, phospholipid peroxidation and protein oxidation accompanied by partial depletion of GSH and impaired GSH/GSSG ratio. Altogether, these changes suggest an initial oxidative stress situation where neurons are unable to counteract the enhanced production of oxidative species. Likely, due to the high levels of oxidative damage markers in brain, the decreased GSH content may regulate downstream

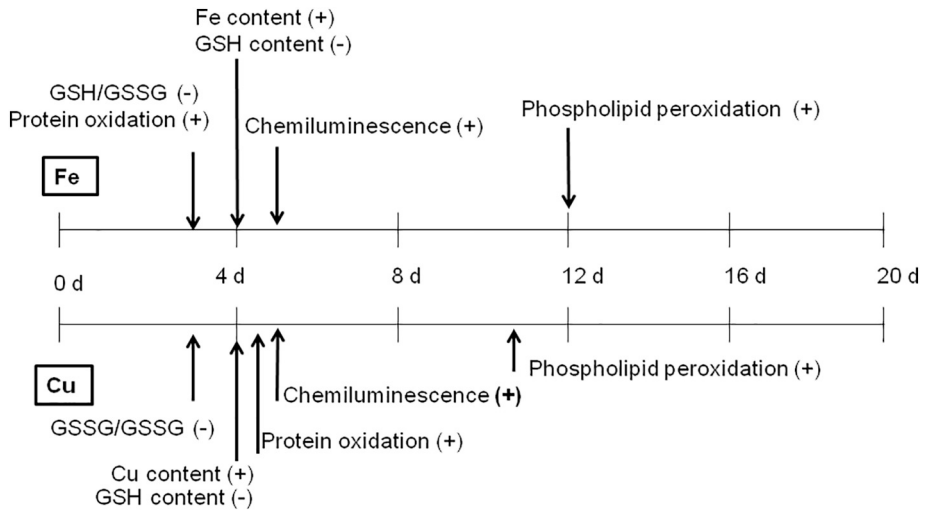

Fig. 8. Kinetics of the brain changes during the initial 20 days of chronic overloads with Fe(II) or Cu(II). The arrows indicate the $t_{½}$, the time to reach one half of the changes in reactions and processes. Increases (+) and decreases (−) are indicated.

effects on metabolism and intracellular signaling regulatory mechanisms that constitute a neuron attempt to protect the organ from metal toxicity, oxidative stress and damage to biomolecules.

Different groups of researchers have reported that Fe and Cu accumulate in the human brain in Alzheimer's and in Parkinson's diseases [33,34]. Through sophisticated and advanced techniques, Szabo et al. [33] were able to determine increased Fe and Cu contents in human frontal cortex. Other metals were also determined in the screening. Whether excess metals appear as a cause or as a consequence of Alzheimer's and Parkinson's diseases is not certain. Wilson's disease patients show increased Cu level in basal ganglia and are characterized and diagnosed by low levels in blood (ceruloplasmin) and high Cu levels in liver. The Cu content of a liver biopsy is the diagnostic criterion for Wilson's disease, values > 250 μg/g dry weight (normal values: < 50 μg/g dry weight) indicate the existence of the disease [35]. Concerning Fe, mitochondrial Fe homeostasis is impaired in neurodegenerative disorders [36].

Brewer has pointed out that the levels of Fe and Cu that are healthy during the reproductive years appear to contribute to the diseases of aging and possibly to the aging process itself with possible effects on cerebrovascular status [37].

The experimental evidence from Fe(II) and Cu(II) overloads in rat brain is immediately examined and challenged by an eventual extension of the observations to the human pathologies associated to these metal dyshomeostasis. However, the extrapolation is not possible. First of all, the homogeneous and continuous experimental data in rats with both metals is at variance with the different human brain function in Fe overload and in Cu overload (Wilson's disease). The human pathology hemochromatosis is characterized by Fe overload, but there is no reported brain dysfunction in this disease. In Parkinson's disease the cerebral accumulation of Fe is not related to hemochromatosis, but presumably a Fe dysmetabolism, and Fe toxicity appears to selectively target mitochondria [38]. Nevertheless, brain dysfunction is a characteristic of Wilson's disease and Cu overload in the brain [38–41].

The neuronal situation after Fe(II) and Cu(II) overloads is of cellular oxidative stress, a condition that establishes a deep change in cell regulation and control. It is not a simple reversible shift of GSH towards oxidation.

Originally, Sies in 1985 defined oxidative stress as a situation with increased oxidative processes or with decreased antioxidant defense [42]. The acceptation of the concept was immediate and it was extensively applied to explain observations and to design new experiments in subcellular systems, cells, tissues and even whole organisms. Recently, Sies updated the concept of oxidative stress for its application and use in redox biology and medicine [43].

Jones redefined oxidative stress as a disruption of redox signaling and control, definition that directs research to the identification of the metabolic perturbations in oxidative stress-related diseases [44], pointed out that cellular macromolecular damage is included in free radical-induced oxidative stress [45], and noticed that large-scale intervention trials with free radical scavenging antioxidant supplements show little benefit in humans [46].

Jones and Sies [47] recently proposed the idea of “redox code” for biological systems as a set of biochemical facts based on the redox positioning of nicotinamide adenine dinucleotides (NAD, NADP), thiol/disulfide systems and thiol redox proteome in a given space and time. The redox code expresses the metabolic organization of aerobic life with a spatiotemporal organization for differentiation, development and adaptation to the environment. Disruption of this metabolic structure during oxidative stress leads to system failure and cellular disease. Sies has recently commented on the present and future of the oxidative stress concept after 30 years of the original proposal [48].

Otero-Losada et al. reported on human oxidative stress considering plasma indicators and antioxidant supplementation in a study with 112 elderly cardiovascular patients. Laboratory data and the clinical response, both indicate moderate improvements, largely depending on the initial condition of the patients [49].

The results presented here clearly show that chronic Fe(II) and Cu (II) overloads in rats lead to brain oxidative stress and damage. Neuronal GSH concentration is the most important antioxidant defense and the ratio GSH/GSSG is a very sensitive indicator of oxidative stress. The ratio GSH/GSSG establishes the cellular redox potential and consequently the whole intracellular redox regulation and control of neuronal metabolism.

Experimental rat models of chronic overloads of Fe(II) and Cu(II) are useful in the understanding of the biochemical mechanisms of toxicity of both metals. In addition, rat models should be useful to develop treatments to prevent the oxidative stress and organ damage in human pathologies associated with iron and copper dyshomeostasis.

5. Conclusion

A neuronal situation of oxidative stress and damage with involvement of oxidative free radical reactions in rat brain is associated with the chronic accumulation of Fe(II) or Cu(I) in the organ. The early decreases in neuronal GSH content and in the GSH/GSSG ratio indicate the central role of GSH in the control of neuronal homeostasis and oxidative processes.

Abbreviations

Aβ	β(beta)-amyloid peptide
APP	amyloid precursor protein
ATP-ase	adenosine triphosphatase
> C = O	carbonyl groups
> C = O*	excited carbonyl groups
DNPH	2,4-dinitrophenylhydrazine
DTNB	5,5′-dithio-bis-(2-nitrobenzoic acid) (Ellman's Reagent)
GSH	reduced glutathione
GSH/GSSG	reduced/oxidized glutathione ratio
GSSG	oxidized glutathione
H_2O_2	hydrogen peroxide
$HO^{\bullet}$	hydroxyl radical
NAD	nicotinamide adenine dinucleotide
NADP	nicotinamide adenine dinucleotide phosphate
NADPH	nicotinamide adenine dinucleotide phosphate reduced
O_2^-	superoxide anion
$^1O_2$	singlet oxygen, the excited state of O_2
ROOH	organic peroxide
$ROO^{\bullet}$	peroxyl radical
ROOOOR	lipid tetroxide (unstable)
-SH	thiol group
TBARS	thiobarbituric acid reactive substances
TNB	2-nitro-5-thiobenzoate

Declaration of Competing Interest

The authors declare that they have no conflict of interests.

Acknowledgements

This study was supported by grants from the University of Buenos Aires (UBACyT 20020170100197BA); the National Research Council of Argentina (CONICET) and the National Agency of Science and Technology of Argentina (ANPCYT) (PICT-2016-002077).

References

[1] S. Rivera-Mancía, I. Pérez-Neri, C. Ríos, L. Tristán-López, L. Rivera-Espinosa, S. Montes, Chem. Biol. Interact. 186 (2010) 184–199, https://doi.org/10.1016/j.cbi.2010.04.010.
[2] M.P. Mattson, Ann. N. Y. Acad. Sci. 1012 (2004) 37–50.
[3] L.M. Sayre, G. Perry, C.S. Atwood, M.A. Smith, Cell. Mol. Biol. (Noisy) 46 (2000) 731–741.

[4] G. Perry, L.M. Sayre, C.S. Atwood, R.J. Castellani, A.D. Cash, C.A. Rottkamp, M.A. Smith, CNS Drugs (2002) 339–352.
[5] W.H. Koppenol, J. Butler, J.W. van Leeuwe, Photochem. Photobiol. (1978) 665-660.
[6] R.J. Ward, D.T. Dexter, R.R. Crichton, J. Trace Elem. Med. Biol. 31 (2015) 267–273.
[7] D.J. Bonda, H.G. Lee, J.A. Blair, X. Zhu, G. Perry, M.A. Smith, Metallomics 3 (2011) 267–270.
[8] J. Becerril-Ortega, K. Bordji, t. Freret, T. Rush, A. Buisson, Neurobiol. Aging 35 (10) (2014) 288–301.
[9] D. Xian-Hui, G. Wei-Luan, S. Tie-Mei, B. Jiang-Tao, Z. Jing-Yi, C. Xi-Ging, J. Trace Elem. Med. Biol. 30 (2015) 118–123.
[10] M.D. Meadowcroft, J.R. Conner, Q.X. Yang, Neurosci. 9 (2015) 225.
[11] M.A. Smith, L.P. Harris, L.M. Sayre, G. Perry, Proc. Natl. Acad. Sci. U. S. A. 94 (1997) 9866–9868.
[12] J.F. Collingwood, R.K. Chong, T. Kasama, L. Cervera-Gontard, R.E. Dunin-Burkowski, G. Peray, M. Posfai, S.L. Siedlak, E.T. Simpson, M.A. Smith, J. Dobson, J. Alzheimers Dis. 14 (2008) 235–245.
[13] O. Weinreb, S. Mandel, M.B. Yodim, T. Amit, Free Radic, Biol. Med. 62 (2013) 52–64, https://doi.org/10.1016/j.freeradbiomed.2013.01.017.
[14] D. Devos, C. Moreau, J.C. Devedjian, J. Kluza, M. Petrault, A. Lalous Jonneaux, G. Ryckewaert, G. Garcon, N. Rouaix, A. Duhamel, P. Jissendi, K. Dujardin, F. Auger, L. Ravasi, L. Hopes, G. Grolez, W. Firdaus, B. Sabbloniere, I. Strubi-Viullaume, N. Zahr, A. Destee, J.C. Corvol, D. Polti, M. Leist, C. Rose, L. Defebvre, P. Marchetti, Z. Cabantchik, R. Bordet, Antiox. Redox Signal 21 (2014) 195–210.
[15] P. Dusek, S.A. Schneider, J. Aaseth, J. Trace Elem. Med. Biol. 38 (2016) 81–92.
[16] W.T. Johnson, Copper and brain function, in: H.R. Liberman, R.B. Kanarek (Eds.), Metal Ions in Life Sci, Chandan Prassad CRC Press, Denton, 2005, pp. 289–305.
[17] A. Kontush, Cell. Mol. Neurobiol. 21 (2001) 299–315.
[18] D. Waggoner, T. Bartnikas, J. Gitlin, Neurobiol. Dis. 6 (1999) 221–230.
[19] A. Ala, A.P. Walker, K. Ashkan, J.S. Dooley, M.L. Schilsky, Lancet 369 (2007) 397–408.
[20] R. Musacco Sebio, N. Ferrarotti, C. Saporito Magriñá, J. Fuda, J, H. Torti, F. Lairión, A. Boveris, M.G. Repetto, J. Inorg. Biochem. 191 (2019) 119–125.
[21] D. Skoog, D. West, F. Holler, Fundamentos de Química Analítica, McGraw-Hill, Mexico, 2014.
[22] A. Boveris, E. Cadenas, R. Reiter, M. Filipkowski, Y. Nakase, B. Chance, Proc. Natl. Acad. Sci. U. S. A. 177 (1980) 347–351.
[23] E. Cadenas, H. Sies, Meth. Enzymol. 105 (1984) 211–230.
[24] J.C. Cutrin, A. Boveris, B. Zingaro, G. Corvetti, G. Poli, Hepatology 31 (2000) 622–632.
[25] B. González Flecha, S. Llesuy, A. Boveris, Free Radic. Biol. Med. 10 (1991) 93–100.
[26] M.G. Repetto, G. Ossani, A.J. Monserrat, A. Boveris, Exp. Mol. Pathol. 88 (2010) 143–149.
[27] C. Fraga, B. Leibovitz, A.L. Tappel, Free Radic. Biol. Med. 4 (1988) 155–161.
[28] A. Reznick, L. Packer, Meth. Enzymol. 233 (1994) 357–363.
[29] R. Musacco-Sebio, N. Ferrarotti, C. Saporito-Magriñá, J. Semprine, J. Fuda, H. Torti, A. Boveris, M.G. Repetto, Metallomics 6 (2014) 1410–1416.
[30] A. Navarro, A. Boveris, Am. J. Physiol. Cell Physiol. 92 (2007) C670–C686.
[31] T.P. Akerboom, H. Sies, Meth. Enzymol. 77 (1981) 373–382.
[32] J. Semprine, N. Ferrarotti, R. Musacco Sebio, C. Saporito Magriñá, J. Fuda, H. Torti, M. Castro Parodi, A. Damiano, A. Boveris, M.G. Repetto, Metallomics 6 (2014) 2083–2089.
[33] S.T. Szabo, G.J. Harry, K.M. Hayden, D.T. Szabo, L. Birnbaum, Toxicol. Sci. 150 (2016) 292–300, https://doi.org/10.1093/toxsci/kfv325.
[34] L.J. Barnham, A.I. Busch, Curr. Op. Chem. Biol. 12 (2008) 222–228.
[35] X. Yang, X. Tang, Y. Zhang, K. Luo, Y. Jiang, H. Luo, J. Lei, W. Wang, M. Li, H. Chen, S. Deng, L. Lai, J. Liang, M. Zhang, Y. Tian, Y. Xu, Hepatology 62 (2015) 1731–1741.
[36] N.P. Mena, P.J. Urrutia, F. Lourido, C.N. Carrasco, M.T. Nuñez, Mitochondrion 21 (2015) 92–105.
[37] G.J. Brewer, Exp. Biol. Med. (Maywood) 232 (2007) 323–335.
[38] M.P. Horowitz, J.T. Greenamyre, J. Alzheimers Dis. 20 (2010) S551–S568.
[39] P. Dusek, T. Litwin, A. Czlonkowska, Neurol. Clin. 33 (2015) 175–204, https://doi.org/10.1016/j.ncl.2014.09.006.
[40] P. Dusek, P.M. Roos, T. Litwin, S.A. Schneider, T.P. Flaten, J. Aaseth, J. Trace Elem. Med. Biol. 31 (2015) 193–203, https://doi.org/10.1016/j.jtemb.2014.05.007.
[41] J. Aaseth, P. Dusek, P.M. Roos, Biometals 31 (2018) 737–747.
[42] H. Sies, Introductory remarks, in Oxidative Stress, H. Sies ed., Academic Press, London, pp. 1–8. doi:https://doi.org/10.1016/B978-0-12-642760-8.50005-3.
[43] H. Sies, Redox Biol. 4 (2015) 180–183, https://doi.org/10.1016/j.redox.2015.01.002.
[44] D.P. Jones, Antiox. Redox Signal. 8 (2006) 1865–1879.
[45] D.P. Jones, Am. J. Physiol. Cell Physiol. 295 (2008) C849–C868.
[46] D.P. Jones, Chem. Biol. Interact. 163 (2006) 38–53.
[47] D.P. Jones, H. Sies, Antiox. Redox Signal. 23 (2015) 734–746, https://doi.org/10.1089/ars.2015.6247.
[48] H. Sies, R.J. Gelpi, A. Boveris, J.J. Poderoso (Eds.), Biochemistry of Oxidative Stress, Springer Internat. Publish, Switzerland, 2016, pp. 3–12.
[49] M. Otero Losada, S. Vila, F. Azzato, J. Milei, Oxidative Med. Cell. Longev. (2013) ID 408260, doi:https://doi.org/10.1155/2013/408260.